Invited Paper
Distributed Optical Fiber Pressure Sensors

Luca Schenato[a,*], Andrea Galtarossa[b,**], Alessandro Pasuto[a], Luca Palmieri[b]

[a] *National Research Council, Research Institute for Geo-Hydrological Protection, Corso Stati Uniti 4, 35127 Padova, Italy*
[b] *University of Padova, Department of Information Engineering, Via Gradenigo 6/B, 35131 Padova, Italy*

Abstract

The measurement of pressure by using distributed optical fiber sensors has represented a challenge for many years. While single-point optical fiber pressure sensors have reached a solid level of technology maturity, showing to be very good candidates in replacing conventional electrical sensors due to their numerous advantages, distributed sensors are still a matter of an intense research activity aimed at determining the most proper and robust pressure-sensitivity enhancement mechanism. This paper reviews early and recent works on distributed pressure sensors, classifying the sensors according to the sensing mechanism. For each type of mechanism, the issues and potentials are analyzed and discussed.

Keywords: optical fiber sensor, distributed optical fiber sensor, pressure measurement, distributed optical fiber pressure sensor

1. Introduction

The measurement of pressure has always been pivotal in many different applications [1, 2, 3], often characterized by the needs of high accuracy, robustness, and dense spatial coverage. As a result, many types of sensor technology have been developed to address the needs of these applications. Among the many, conventional electrical sensors such as load cells, piezometers, and capacitive sensors are the most popular, especially for pressure sensing in liquid. However, these electrical sensors are unsuitable for long-range monitoring, as they are sensitive to electromagnetic interference (EMI), and cannot be easily multiplexed in a large sensor network.

Single-point fiber optic sensor technologies have been proposed as solutions for pressure sensing for many years. At present, some single-point fiber pressure sensors, e.g., Fiber Bragg gratings (FBGs) [4, 5, 6, 7] and interferometric-based ones [8, 9], have already been released as commercial products due to the many features, such as minimal invasiveness, remote powering and interrogation, multiplex capability, and roughness. In particular, they can also work in high-temperature environments [10, 11], also due to the technology improvement in FBG writing [12, 13, 14]. Nonetheless, there are still applications for which the spatial resolution attainable with single-point fiber optic sensors is not enough, such as in the geo-hydrological sector [15] and oil&gas industry [16]. Indeed, single-point fiber sensors, even when densely multiplexed into quasi-distributed fiber sensors, cannot provide the wealth of information that may come from distributed optical fiber sensors (DFOSs).

Although the pressure has been one of the first physical field addressed by the researchers' efforts towards the development of specific distributed optical fiber sensors, to date, these have not yet delivered the required reliability for the commercialization. Nowadays, there is an increased and renovated interest in the development of distributed pressure sensors (DPSs), boosted by the potential applications and by the growing availability and reliability of high resolution distributed strain sensing schemes.

This review paper aims at discussing the key concepts of distributed fiber optic pressure sensors and reviews the more recent results. The different approaches adopted so far to enhance the pressure sensitivity are outlined, emphasizing the sensing mechanism. Each solution is compared in terms of pressure sensitivity, resolution, and, when possible, temperature cross-talk. Finally, open issues and future perspectives are analyzed.

Guide to the reading

The response of an optical fiber to a pressure field can be divide into three different regimes depending on the frequency of the applied pressure [17], as shown in Fig. 1. For frequencies below about 10 kHz, we have the *hydrostatic* regime, in which both axial and radial strains contribute to the pressure sensitivity of the fiber. Above this threshold and up to about 1 MHz, the pressure has only a radial effect, and the fiber length is almost constant. Finally, for higher frequencies, the wavelength of the pressure field becomes comparable to the fiber diameter, and the induced strain depends on the direction of propagation of the pressure wave. As a result, the induces stress

*Corresponding author
**Co-corresponding author
Email addresses: luca.schenato@cnr.it (Luca Schenato), andrea.galtarossa@unipd.it (Andrea Galtarossa)

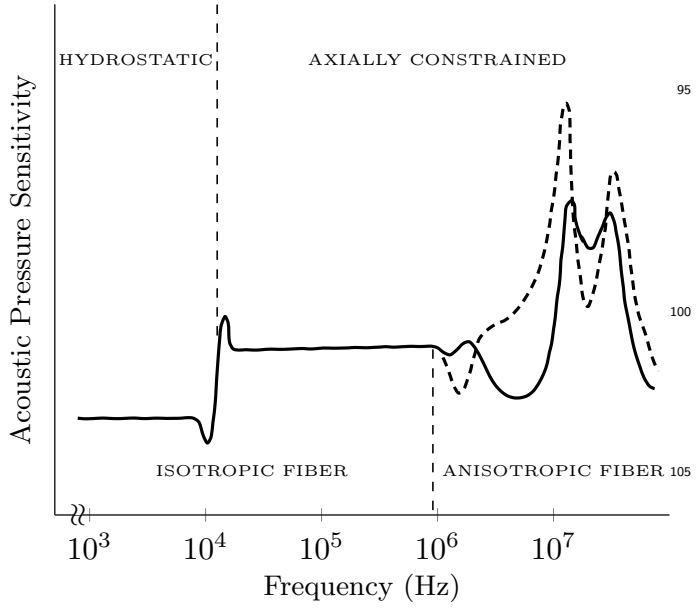

Figure 1: Pressure response of a single mode fiber at different frequency regimes. Data from [17].

field is asymmetric, and the fiber becomes anisotropic and birefringent. In this work, we will focus on the hydrostatic regime.

Unfortunately, uncoated optical fibers are almost insensitive to hydrostatic pressure [18, 19] and, therefore, its direct measurement by merely exposing the fiber to the pressure field cannot achieve high sensitivity. Thus, over the years, the research has focused on developing transducing mechanisms that can effectively convert pressure into another physical parameter–typically strain or birefringence. This approach, originally conceived for single-point or integral optical fiber sensors, is nowadays adopted also for distributed optical fiber sensors. Among the different standpoints that can be chosen to explore DPSs, we have opted to classify them on the basis of the sensing mechanisms. A simpler classification could be based on the acquisition technique, but this would not be informative given that what impacts the performance of the sensor is the transducing mechanism, rather than the interrogation technique. Therefore, we can conveniently distinguish the following three main categories:

- measurement of pressure-induced strain in compliant coated optical fibers and engineered cables;
- measurement of pressure-induced birefringence in special optical fibers;
- measurement of pressure-induced losses in special optical fibers;

while keeping the classification based on the acquisition technique, within the first two categories.

In the following, each category will be extensively described and discussed; a great effort has been spent to include as many significant references as possible, but at the same time, we are aware that some might have been overlooked.

2. Measurement of pressure-induced strain in compliant coated optical fibers and engineered cables

Direct pressure exposure induces changes in the optical fiber properties in different ways: by modifying the index of refraction of the material, by inducing strain along the direction of light propagation and by modifying the waveguide dispersion [20]. The earliest works addressing this topic focused mainly on the pressure-induced change of the refractive index. In 1978, Shajenko et al. [21] suggested that the contribution of pressure-induced longitudinal strain may be comparable to pressure-induced refractive index modulation effect, while, one year later, Hocker [20] showed that the contribution of waveguide dispersion is negligible compared to the other two effects. Bucaro and Hickman also drew a similar conclusion [22]. Both the works of Shajenko and Hocker assumed a bare fiber subjected to hydrostatic compression, while the work of Bucaro and Hickman assumed only a radial compression (i.e., no pressure is applied at the fiber ends).

Bucaro et al. also demonstrated that the sensitivity of an optical fiber hydrophone to acoustic pressure could be greatly enhanced by using a polymer-clad optical fiber rather than an unclad fiber [22, 23, 24, 25]. Later, Budiansky et al. [18] showed analytically that this occurs when the coating is much more compressible than the fiber. In particular, they provided an expression for the relative phase-delay change

$$\frac{\Delta\phi}{\phi} = \varepsilon_{zg} - \frac{n^2}{2}\left[2\varepsilon_{rg}(p_{11}-p_{44}) + \varepsilon_{zg}(p_{11}-2p_{44})\right] \quad (1)$$

experienced by light as a consequence of the applied pressure. In this formula, $p_{11} \approx 0.13$ and $p_{44} \approx -0.075$ are two components of the photoelastic Cartesian tensor of fused silica glass, n is the refractive index, ε_{zg} and ε_{rg} are the axial and radial components of the induced strain, respectively. The latter quantities depend on the diameter of the glass fiber, a, and of the polymer coating, b, and their respective Young's moduli, E_g and E_p, and Poisson's ratios, ν_g and ν_p. Typically, $E_p \ll E_g$ and also assuming that $f = (a/b)^2 \ll 1$, where b is the radius of the clad fiber and a the radius of the unclad fiber, the strain components read

$$\varepsilon_{zg} \approx -\frac{1-2(1-f)\nu_p - 2f\nu_g}{fE_g + (1-f)E_p}p \quad (2)$$

$$\varepsilon_{rg} \approx \left[\frac{\nu_g(1-2\nu_p) - f(1-\nu_g-2\nu_g\nu_p)}{fE_g+(1-f)E_p} - \frac{(1+\nu_g)(1-2\nu_g)(1-f)E_p/E_g}{fE_g+(1-f)E_p}\right]p. \quad (3)$$

Note that, owing to Eq. (1), the axial strain ε_{zg} generates two phase-delay contributions that are opposite in sign;

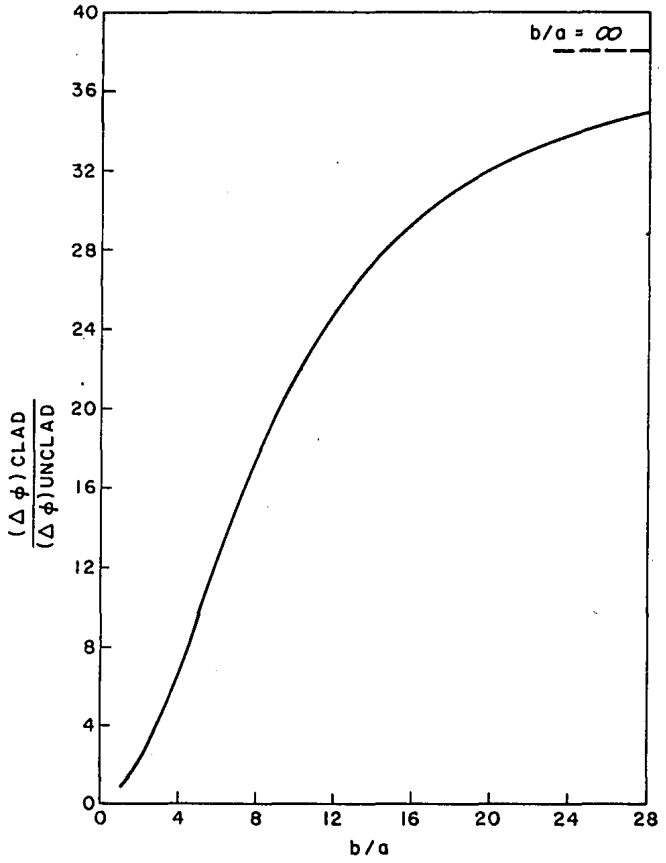

Figure 2: A calculation of $\Delta\phi_{\text{clad}}/\Delta\phi_{\text{unclad}}$ as a function of the ratio b/a between the radius b of the clad fiber over the radius a of the same fiber when unclad. Reprinted with permission from [18] ©The Optical Society.

the first stems from the geometrical axial deformation of the fiber, the second from the associated elasto-optic effect. Moreover, note also that, according to Eq. (2) and depending on the values of f, ν_p and ν_g, a positive pressure p may induce a negative axial strain, i.e. a fiber compression. Counter-intuitive as it is, this is actually what typically happens in coated fibers, and it has also been observed in cables with a more complex cross-section, like submarine optical fiber cables [26].

Following the above analysis, Budiansky et al. concluded that the pressure sensitivity of a bare unclad optical fiber is about -2.2×10^{-6} MPa^{-1} and, most importantly, this sensitivity can be boosted up to a factor of larger than 30 with a very thick polyethylene coating (see Fig. 2).

The work of Budiansky et al. was then greatly expanded by Hughes and Jarzynski [27], which provided a solution of the elastostatic equations for a multilayered fiber under hydrostatic pressure. They confirmed that the main factor that controls the induce phase change is given by the longitudinal strain, whereas the contribution of radial strain is generally negligible for most of the common materials used for coatings.

Following a similar procedure, Lagakos and co-authors demonstrated analytically that, by properly choosing the

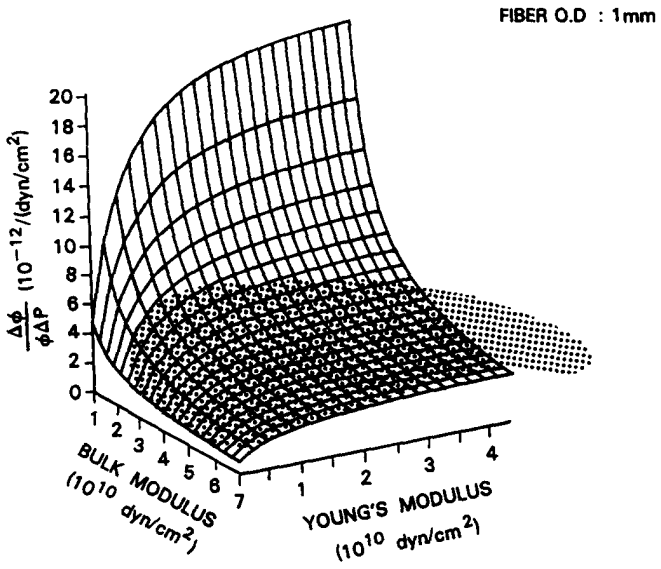

Figure 3: Low-frequency hydrostatic pressure sensitivity vs. Bulk and Young's Moduli of the Outer Coating of a Single-Mode Fiber (10^{10} dyn/cm^2=1 GPa). Reprinted with permission from [17] ©Elsevier.

glass and coating materials, and the corresponding thicknesses, it is possible to have optical fibers with reduced pressure sensitivity [28], or even insensitive to the pressure field [29, 30]. They also analyzed the pressure sensitivity of an optical fiber with an inner coating of silicone as a function of the external outer coating and for different frequencies [31, 32, 17]. At low frequency (< 1 kHz), they confirmed that both the axial and radial strains contribute to the fiber's sensitivity, with the most substantial contribution coming from the axial strain. The sensitivity is generally governed by both the bulk and Young's moduli of the outer coating material: the bulk modulus, which is the inverse of compressibility, determines the maximum dimensional changes of the coating in response to the external pressure. In contrast, Young's modulus controls the effectiveness of the strain transfer from the coating to the fiber itself. Therefore, they concluded that an enhanced hydrostatic pressure sensitivity could be attained with a coating having low bulk modulus and high Young's modulus, as shown in Fig. 3. Regarding the coating's thickness, for thick coatings, the pressure sensitivity is directly proportional to the compressibility of the coating; therefore, having a low bulk modulus coating is to be preferred as it provides large sensitivity. Examples of such material are the polytetrafluoroethylene (PTFE) and the fluorinated ethylene propylene (FEP). Conversely, for thin coatings, high Young's coefficient materials (such as Noryl™) should be preferred, even if characterized by intermediate bulk modulus.

2.1. Brillouin-based distributed sensing

All the works mentioned above are explicitly focused on integral phase-modulation pressure sensors; yet, they

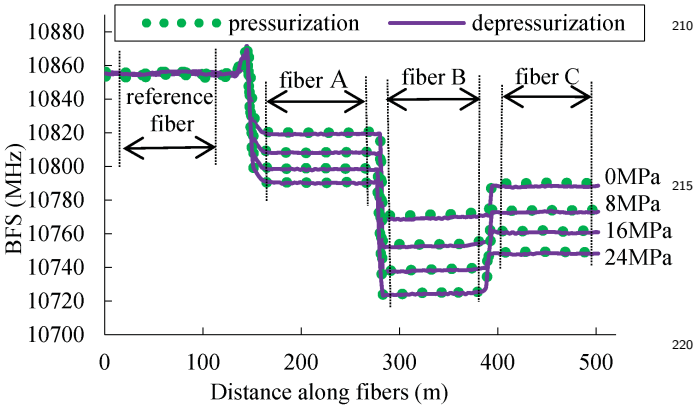

Figure 4: Brillouin frequency shift along three different double-coated test fibers under different pressures. Outer coating Young's moduli are 0.75, 0.75 and 0.55 GPa, respectively; Poisson's ratios are 0.465, 0.465 and 0.455, respectively and coating radii are 250, 450 and 450 µm respectively. The pressurization and depressurization curves overlap very well to testify that there is no significant hysteresis. ©2020 IEEE. Reprinted, with permission, from [35].

provide general conclusions and models that have also been exploited for distributed pressure sensors, which use strain as a proxy for pressure. As well known, distributed strain measurement can be obtained by exploiting Brillouin or Rayleigh scattering. Remarkably, interferometric strain sensing schemes may provide large strain sensitivity [33], but they are not distributed, and multiplexing of those sensors are quite cumbersome and limited to a few sensors.

In one of the first works using Brillouin, Méndez and Diatzikis [34] investigated a fiber with a special coating combination of Nylon and silicone layers and an outside diameter of 1.2 mm. The fiber was exposed to increasing hydrostatic pressure in a high-pressure stainless steel vessel and interrogated with a commercial Brillouin optical time-domain reflectometer (BOTDR) at 1.55 µm. The reported pressure sensitivity is −3.34 MHz/MPa (expressed in term of Brillouin frequency shift, BFS, per unit pressure), with a ten- and five-fold enhancement with respect to an uncoated fiber (−0.38 MHz/MPa) and a standard SMF-28 fiber (−0.74 MHz/MPa), respectively. Similarly, in [35] three engineered fibers with double-layer coatings were characterized, showing pressure sensitivities of −1.27, −1.91 and −1.67 MHz/MPa, respectively, corresponding to an enhancement of 1.7, 2.6 and 2.3 times with respect to standard silica fiber (Fig. 4).

The Brillouin pressure sensitivity of standard single-mode fibers has been characterized by several Authors, with slightly varying results. Le Floch and Cambon [36] estimated a sensitivity of −0.91 MHz/MPa, Gu et al. [37, 38] reported different values ranging from −0.7432 MHz/MPa and −0.752 MHz/MPa. The difference in these values might be due to the different fibers coatings, which were, however, not specified. In [37], the Authors also analyzed how the sensitivity is affected by straining the fiber, showing that when the fiber is pre-tensioned before pressurization, the sensitivity decreases to −0.412 MHz/MPa; this fact was imputed to the different dependence of the BFS on the pressure-induced radial and axial strain.

The pressure-induced BFS in polymer optical fibers (POF) has also been investigated [39]. Differently from silica optical fibers, BFS increases with pressure. According to the Authors, this stems from two factors, the increased density of the polymer material due to pressure, leading to increased acoustic velocity, and the negative dependence of polymer Young's modulus on the pressure-induced axial strain. Moreover, since polymers are typically softer than silica glass, the pressure-induced BFS and hence the sensitivity is larger. Nonetheless, a pre-treatment is required to contrast the hysteresis that usually occurs. The Authors in [39], considered a perfluorinated graded-index polymer fiber (PGFI POF) and found that at least three pressure cycles are required to stabilize the pressure response and, at the end of the process, the sensitivity was 4.3 MHz/MPa, approximately six times larger, in modulus, than standard silica fibers.

2.2. Rayleigh-based distributed sensing

Historically, Rayleigh-based distributed sensing systems were the first to be proposed, and already in the late '80s A. J. Rogers envisaged the potential of these systems in measuring pressure [19]. In particular, he calculated that a pressure of approximately 0.1 MPa should produce a phase shift equivalent to 1 µε.

Becker and co-authors investigated the use of fiber-optic distributed acoustic sensing (DAS) to measure the oscillatory strain rate along a standard fiber-optic cable caused by pressure waves at mHz-frequencies [40]. The experiment was carried out in a water-filled reservoir subjected to a controlled oscillating water level.
The DAS, with a spatial resolution of 10 m and a sampling distance of 0.25 m, was connected to about 200 m of tight-buffered (900 µm diameter) single-mode optical fiber, wrapped around a 10 cm diameter PVC pipe and submerged in the water reservoir. To avoid any contribution to the strain from the PVC pipe deformation, a layer of nylon mesh was interposed between the fiber and the tube surface. Due to the DAS capability of measuring only dynamic strain, this work dealt with dynamic hydrostatic pressure oscillating with periods of 10, 100, 500, and 720 s (equivalent to a frequency of 100, 10, 2 and 1.4 mHz, respectively) and amplitudes of 40, 100, 500, and 1000 Pa. The measured strain-rate was integrated over time to obtain the pressure-induced strain, and the raw data was processed by filtering and averaging (over 75 m of fiber). The amplitudes were extracted by fitting a sine function to the filtered signal through nonlinear regression. A summary of the strain vs. pressure curves is shown in Fig. 5. The response increased with the frequency of the oscillating waves, with a pressure sensitivity that decreased with the oscillating period and was, at best, 8.1×10^{-4} nε/Pa for the pressure waves at the shorter period. The Authors also highlighted that they do not have a clear explanation for the decreasing of sensitivity

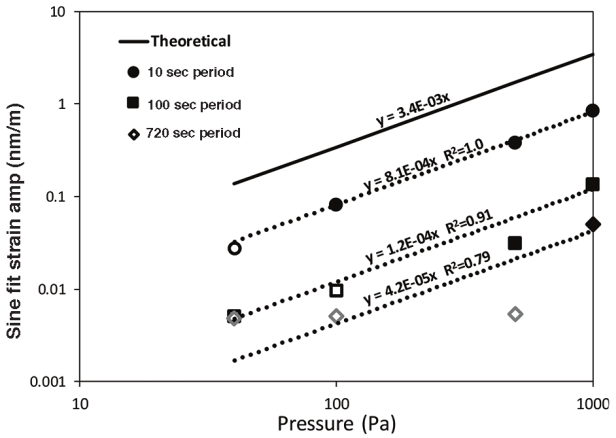

Figure 5: Summary of strain responses vs. pressure oscillation amplitudes measured by using a DAS. Open symbols represent measurements with a bad sinusoid fitting. Open gray symbols correspond to no detectable sinusoidal signal. Trend lines (with regression equation) are shown as dashed lines. A theoretical guess based on Young's modulus of 73 GPa and Poisson's ratio of 0.25 for glass fibers is shown as a solid line. Republished with permission of Society of Exploration Geophysicists (SEG), from [40]; permission conveyed through Copyright Clearance Center, Inc.

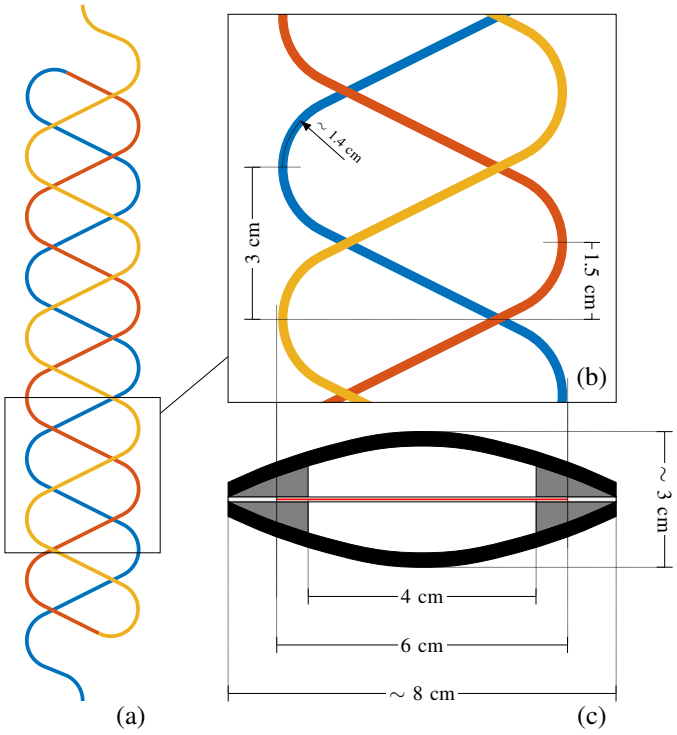

Figure 6: A DPS cable design: (a) the meandering path of the three fibers embedded in the cable; (b) magnified view of the path. (c) The cable cross-section. ©2020 IEEE. Reprinted, with permission, from [41].

at longer periods, although a tentative explanation may be found in the pressure dependence of Young's modulus of the coating, as shown in [31]. Ultimately, the tests showed that this approach works for hydrostatic pressure waves with short oscillation periods (<10 s) and pressures as small as 100 Pa but with lower sensitivity than piezoelectric transducers.

A different approach to increase pressure sensitivity consists of engineering the cable housing the fiber, rather than its coating. This idea has been recently explored in Ref. [41], where a high-sensitive, high-spatial-resolution distributed pressure sensing cable, employing standard single-mode fibers, has been proposed. The cable structure has been opportunely designed to transfer the external pressure into an elongation of the fiber. As shown in Fig. 6, the cross-section of the cable is constituted by two arched rubber profiles that enclose an elastic band embedding the fiber, which is deployed according to a meandering path. By squeezing the structure, the pressure pulls the elastic band and the embedded fiber in the transverse direction. Noticeably, this cable design is compliant with any optical fiber distributed strain sensing technique.

The cable sensitivity and spatial response were characterized by a commercial optical frequency domain reflectometer (OFDR). In particular, the spatial response was assessed considering not only the optical resolution of the interrogator but also (and prominently) the mechanical transfer function of the cable [42]. This procedure that should also be applied to any high-thickness coated cable and any other distributed optical fiber sensors, in general. The work also shows, by an accurate characterization and proper data analysis, the effect of the mechanical response of the cable can be partly compensated, improving the spatial resolution (see Fig. 7). In particular, the cable showed an intrinsic spatial resolution of about 8.5 cm, with a mean sensitivity of −30 GHz/kPa. With 150 MHz of spectral shift resolution, the pressure resolution was approximately 5 Pa, while the root-mean-square accuracy was limited to 5 hPa, mainly due to cable manufacturing imperfections. Finally, we remark that the pressure sensitivity offered by this cable with respect to the spectral shift resolution of the interrogation system is about three to four orders of magnitude higher than that achieved by merely engineering the fiber coating (according to the results reported in Sec. 2.1 and assuming a spectral shift resolution in the order of 1 MHz for Brillouin systems). Moreover, by varying the geometrical parameters (thickness, width, etc.) and changing the material, the sensitivity of this cable design can be tuned over a wide range of values.

To facilitate the Reader, we have summarized the specifications of the DPSs, which exploit the measurement of pressure-induced strain, in Table 1.

3. Measurement of pressure-induced birefringence in special optical fibers

The idea of measuring polarization variation along the fiber for sensing several parameters, including pressure, dates back to 1980 when A.J. Rogers [43, 44] proposed the use of the polarization optical time-domain reflectometry

Table 1: Distributed pressure sensors exploiting the measurement of pressure-induced strain.

Ref.	Tech.	Distance		Fiber		Pressure			
		Resol. [m]	Range [m]	Type	Coating	Sensit. [MHz/MPa]*	Resol. [MPa]*	Range [MPa]*	Accur. [kPa]
[34]	BOTDR	2†	20	SMF	1.2-mm nylon	-0.74	0.467	34.5	2000†
					1.2-mm silicone	-3.34	0.103		
[35]	BOTDA	5	500	n.a.	250 µm ETFS	-1.27	1.57	24	n.a.
					450 µm ETFS	-1.91	1.05		
					450 µm Hytrel	-1.67	1.20		
[36]	BOTDA	n.a.	500	SMF	n.a.	-0.91	n.a.	25	n.a.
[38]	BOTDA	5	500	Corning SMF28e+		-0.7457	2.68	28	n.a.
				YOFC G652.D		-0.7432	2.69		
[39]	BOTDA	n.a.	3	PFGI POF		4.3	n.a.	0.6	n.a.
[40]	DAS	10	200	SMF	tight buffer	0.81 nε/kPa @ 0.1 Hz	40 Pa‡	1 kPa	n.a.
[41]	OFDR	0.085	1	G.657	engineered cable	−30 GHz/kPa	5 Pa	1 kPa	0.5

* Unless otherwise specified
† Determined from the instrument datasheet
‡ Minimum detectable pressure

(POTDR), which happens to be the first documented distributed optical fiber sensor ever proposed [45]. The idea of measuring pressure through the birefringence it induces was subsequently exploited and explored in several works, using not only Rayleigh but also Brillouin scattering.

3.1. Rayleigh-based systems

One of the earliest approaches consisted in the exploitation of the pressure-induced birefringence, or its variation, in dedicated high-birefringence special fibers. The enhanced pressure sensitivity of such fibers has been investigated since the late 80s'. Xie et al. [46] studied some special birefringent fibers, known as side-hole fibers (SHF), whose structure is similar to that of the PANDA fibers, except that the bores where the stress-applying rods should be inserted are left empty (see Fig. 8). Since the material is uniform, the birefringence of SHFs is less sensitive to temperature. Their simple structure makes manufacturing and splicing easier, and they can be either exposed to a pressure acting on the external surface or inside the bores.

The fiber studied in that work has an outer diameter $2b = 190\,\mu\text{m}$, bores diameter $2r_0 = 58\,\mu\text{m}$, a combined wall thickness of either side of the fiber $w = b - 2r_0 = 37\,\mu\text{m}$. The Authors provided an analytical expression for the pressure-induced birefringence B based on a plane-wave approximation on a square model of the fiber, given by:

$$B = \beta_x - \beta_y = \pm S\,p, \tag{4}$$

$$S = -2\,p_{44}\frac{1+\nu_g}{E_g}\,\frac{\pi n_0^3 b}{\lambda w}, \tag{5}$$

where S is the pressure sensitivity for pressure p, β_x and β_y are the propagation constants of x- or y-polarized light, λ the free-space wavelength, n_0 the mean refractive index, and the other parameters have been defined above. The sign in Eq. (4) is negative when the pressure is applied inside the bores, and positive for external pressure. The calculated sensitivity for such silica SHF at $\lambda = 633\,\text{nm}$ was $S \simeq 96\ \text{rad}\,\text{m}^{-1}\,\text{MPa}^{-1}$. The experimental characterization confirmed the sensitivity with good accuracy ($S = 102$ and $110\ \text{rad}\,\text{m}^{-1}\,\text{MPa}^{-1}$ for internal or external pressure, respectively). Most important, Eq. (5) shows that the sensitivity S of the SHF is driven by the factor b/w, which may be considered the pressure-transducing gain of the fiber: the thinner the walls of the holes, the larger this gain, within the limit of fiber mechanical integrity. Consistent conclusions were also achieved in [47].

The pressure sensitivity of standard bow-tie fibers has been investigated, too. Chiang et al. [49, 50] carried out an extensive analytical study about the pressure sensitivity of such fibers and the possible contribution of coating, finding that sufficiently thick coating with desired elastic properties can significantly increase the pressure-induced birefringence. He also considered the case of a pure radial pressure condition, theoretically showing that the pressure-induced birefringence in the fiber is determined mainly by the elastic properties of the fiber glasses and is rather insensitive to the coating material and thickness [51].

Another fibers that have been extensively investigated as pressure sensors are the photonic crystal fibers (PCFs). For example, Szpulak et al. [52] calculated the sensitivity of both phase and group modal birefringence to the hy-

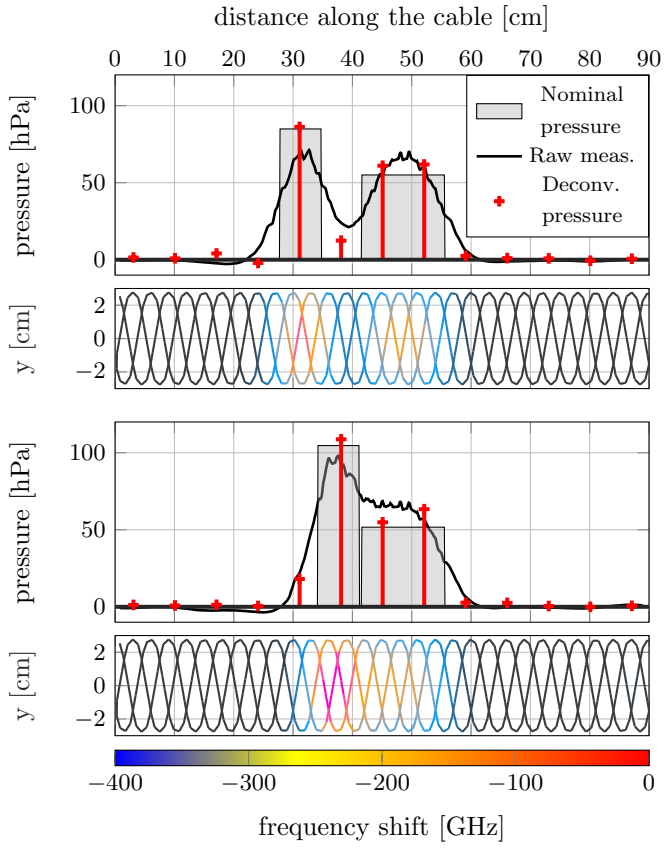

Figure 7: Distributed pressure measurements performed in two different configurations with the DPS cable of Fig. 6. Upper graphs show the nominal pressure distribution (gray areas), the raw pressure measurements obtained considering only the cable sensitivity (black curves), and the distributed pressure measurements obtained by the spatial deconvolution (red stems). Lower graphs show the frequency shift measured along the fibers mapped along the cable. ©2020 IEEE. Reprinted, with permission, from [41].

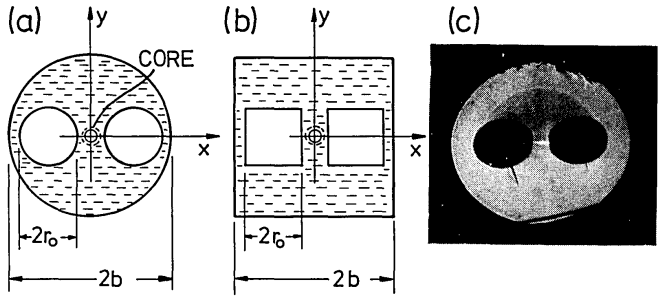

Figure 8: (a) Cross-section of the SHF proposed in [46] and characterized by a enhanced pressure-induced birefringence. (b) Square model of the SHF, used for approximate calculation. (c) Experimental fiber cross-section: approximate dimensions $2b = 190\ \mu$m; $2r_0 = 58\ \mu$m. Reprinted with permission from [46] ©The Optical Society.

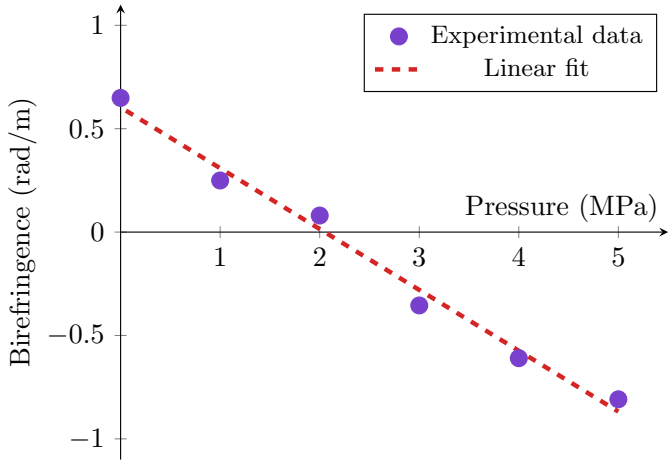

Figure 9: Birefringence vs pressure in a SHF, measured with a PODTR scheme. Data from [48].

drostatic pressure of two birefringent PCFs numerically. They separately analyzed the contribution of the geometric effects (i.e., the deformation of the inner holey pattern) from that due to the stress, finding that their contributions to the phase and group birefringence are synergistic. The more significant contribution is imputable to the stress-related effects, while the geometrical deformations contribute only marginally to the overall pressure sensitivity value. They also highlighted that the pressure sensitivity achievable with the PCFs is smaller than that of SHFs (up to one order of magnitude smaller). Nonetheless, the PCFs analyzed in that work had a lower cross-sensitivity to temperature with respect to SHFs (370 °C/MPa vs. 200 °C/MPa, meaning that in the PCF a pressure variation of 1 MPa has an effect equivalent to a temperature variation of 370 °C). This was also confirmed experimentally, for other high birefringent PCFs [53].

One of the first publications about a distributed pressure measurement exploiting an SHF interrogated by a POTDR is again from A.J. Rogers [48]. The SHF used in that work included two bores on the sides of the single-mode core. Due to the bores, any significant pressure compresses the core region asymmetrically, causing stress birefringence proportional to the pressure difference between the outside surface and the inner bores. The experimental results are shown in Fig. 9, where it is interesting to note that the pressure-induced birefringence tends to cancel the intrinsic fiber birefringence. This required a full polarimetric inversion of the collected data, to retrieve the sign of the pressure-induced birefringence; the analysis can be however simplified if the intrinsic birefringence is large enough to avoid the zero crossing. The spatial resolution of the setup was about 1 m over distances of tens of kilometers; the measurement time was in the order of minutes.

Some years later, Chen et al. [54] proposed a polarization-maintaining photonic crystal fiber (PM-PCF) and an SHF fiber interrogated by a polarization optical frequency-domain reflectometer (POFDR). The first fiber was an all-silica PM-PCF from Blaze Photonics (PM-1550-01), with pitch 4.4 µm, hole diameter 2.2 µm, and large hole diameter 4.5 µm. The cladding diameter of the fiber is

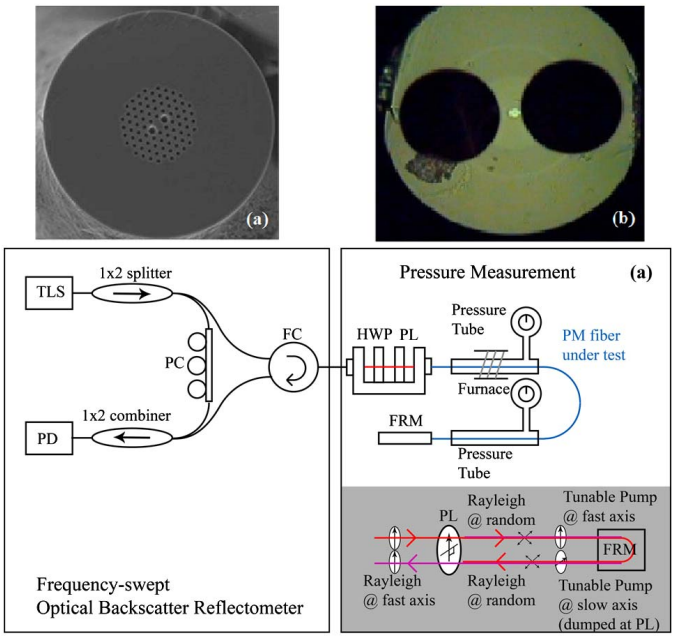

Figure 10: Upper pictures: cross-sections of a PM-PCF (on the left), and a SHF (on the right) used in [54] for pressure sensing with a POFDR. Lower scheme: Experimental setup of the POFDR, used to interrogated the fibers above, which allows to probed both polarization axis: TLS, tunable laser source; PD, photodiode; FC, fiber circulator; HWP, half-wave plate; PL, polarizer; FRM, Faraday rotation mirror; PM fiber, polarization-maintaining fiber. Reprinted with permission from [54] ©The Optical Society.

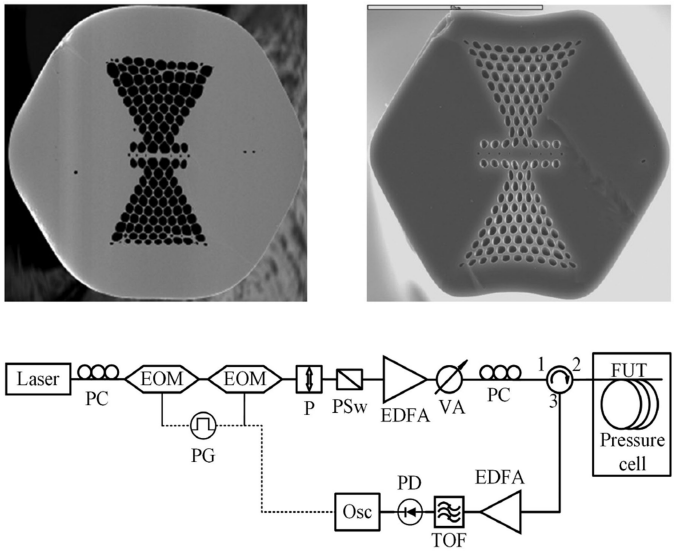

Figure 11: Upper pictures: cross-section of two highly birefringent "Butterfly" photonic crystal fibers used in [58] for pressure sensing with a Φ-OTDR. Lower scheme: Experimental Φ-OTDR setup used for the distributed pressure measurement: EOM, electro-optical modulator; PC, polarization controller; PG, pulse generator; P, polarizer; PSw, polarization switcher; EDFA, Erbium-doped fiber amplifier; VA, variable attenuator; Osc, oscilloscope; PD, photodiode; TOF, tunable optical filter; FUT, fiber under test. ©2020 IEEE. Reprinted, with permission, from [58].

125 µm, while the holey area has a diameter of about 40 µm. The second fiber had an outer diameter of 220 µm with two symmetric air holes with diameter 90 µm. The core, 9.7 × 7.5µm in size, is horizontally aligned with the air holes, and vertically shifted of 4.5 µm with respect to the geometric center of the fiber. In this work, pressure-induced birefringence is calculated from the difference between Rayleigh spectral shifts of the two orthogonal polarizations supported by the fibers and measured using the scheme described in [55]. This scheme, by terminating the probed fiber with a Faraday rotating mirror, allows measuring the Rayleigh spectral shifts of the two orthogonal polarizations one after the other, as if they were concatenated (with the second polarization probed in the backward direction), as shown in Fig. 10. The pressure sensitivity was estimated as the differential strain per unit of pressure measured on the two polarizations. The fibers, 2 m in length, showed a pressure sensitivity of 3.48 µε/MPa (equivalent to −0.522 GHz/MPa) and 12.5 µε/MPa (equivalent to −1.874 GHz/MPa) over a range of 0–13.8 MPa for the two types of fibers,respectively. Despite the short length of these fibers, the measurements were carried out with a commercial interrogator with 1 cm of spatial resolution, potentially allowing the measurement over fibers up to 70 meters long, with a strain resolution of 1 $\mu\varepsilon$ (i.e., 150 MHz of Rayleigh spectral shift).

Gerosa et al. [56] proposed to use an embedded-core fiber (ECF) consisting of a capillary tube with a germanium-doped core embedded in its sidewall. When pressure is applied, an asymmetric stress distribution is induced into the core, giving rise to birefringence variations. These were measured using an OFDR by exciting both polarizations at the same time. In this way, the induced birefringence manifests as a pair of symmetric peaks in the autocorrelation of the trace spectrum [57]. The ECF used in this work was only 77-cm-long, interrogated with the same commercial interrogator used in the previous work, over a pressure range of 0–24 MPa. The measured sensitivity was approximately −0.499 GHz/MPa, showing a marginal improvement over the pressure sensitivity of a commercial photonic crystal fiber (PM-1550, from NKY Photonics) measured at −0.394 GHz/MPa in the same paper.

Mikhailov et al. [58] characterized two highly birefringent "Butterfly" photonic crystal fibers, using a frequency scanning Φ-OTDR , with which the Rayleigh spectral shift could be measured with a resolution of 64.5 MHz (Fig. 11). The setup could probe each of the polarization axes of the fiber using a polarization switch and controller; the spatial resolution is 5 cm over a distance range of some kilometers. The butterfly PCFs (shown in the upper pictures of Fig. 11) are by design almost temperature and strain insensitive and have a relatively high loss coefficient of 24 dB/km; therefore, the samples used in the experiments were only 26.5 m and 48 m long.

The proposed method consists of measuring the birefringence variations with respect to a reference measurement taken at a reference pressure. Subsequent pressure

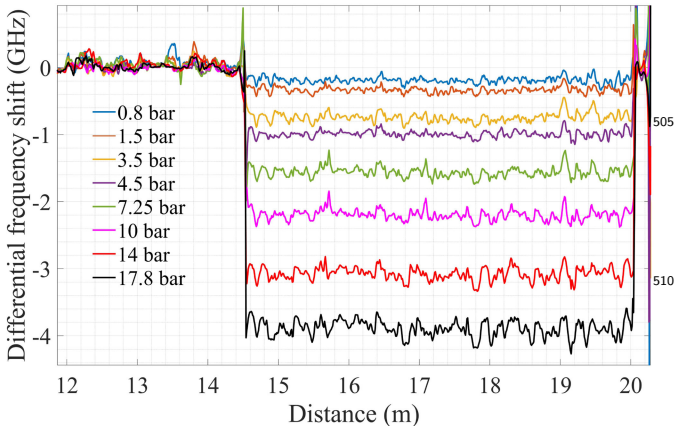

Figure 12: Differential frequency shift pressure response between the two polarization axes of the "Butterfly" PCF shown in the upper left picture of Fig. 11. ©2020 IEEE. Reprinted, with permission, from [58].

variations induce changes in the refractive indices $\Delta n_{s,f}$ of the slow and fast polarization axes of the fiber, respectively. These variations are related to the measured shifts $\Delta\nu_{s,f}$ by [57]

$$\Delta n_{s,f} = \frac{n_{s,f}}{\nu_0}\Delta\nu_{s,f} \tag{6}$$

where $n_{s,f}$ are the refractive indices of the polarization axes at reference state and ν_0 is the central frequency of the scanned band. The resulting birefringence variation is then given by $\Delta B = \Delta n_s - \Delta n_f$.

A portion of 5.5 m of each fiber was probed in an oil pressure chamber, where the pressure was varied over the range 0–6.8 MPa; as an example, the pressure response of the first fiber is shown in Fig. 12. The measured pressure sensitivities for the two fibers were −2.19 GHz/MPa and −0.954 GHz/MPa; the setup offers a resolution up to 0.03 MPa for the fiber with the larger sensitivity, and uncertainty of 2.2 MPa and 5.9 MPa for the two fibers, respectively. Noticeably, the same group tested the same approach with low-losses SHFs, up to 1.05 km long [59].

3.2. Brillouin-based systems

Another distributed sensing technique that exploits PM fiber is based on the generation of the so-called Brillouin Dynamic grating (BDG), which are created by stimulated Brillouin scattering. In detail, the interaction of two counter-propagating pump waves generates and sustains a localized acoustic wave in the fiber–i.e., the BDG; this can be probed by a third light signal that generates Brillouin scattering at the frequency shift related to the fiber local temperature and strain. The position of the BDG along the fiber can be varied by controlling the relative delay of the pumps. Most applications of BDG exploit a high-birefringence PM fiber, where two pumps are launched onto one polarization axis to create the BDG, and the probe wave is launched into the other polarization axis. The reflection at the BDG is maximum when the frequency difference between the co-propagating probe and pump waves satisfies the phase matching $\Delta\nu_{BireFS} = \Delta n\,\nu/n_g$, where Δn is the phase birefringence, n_g is the group refractive index, and ν is the frequency of probe wave. Therefore, a distributed measurement of the birefringence is achieved by probing the BDG reflected frequency, and, as done for the works above on POTDR and POFDR, the local birefringence can be used as a proxy to measure the pressure field.

A first work, yet only numerical, that proposed the exploitation of the generation and interrogation of BDGs for distributed pressure sensing came from S. Nouri Jouybari et al. [60]. In this work, a numerical analysis was performed considering an SHF with core-, holes- and fiber-radius of 3, 15, and 60 µm, respectively. The distance of the holes from the fiber center was 20 µm, and the core of the fiber was doped by 3.5% in weight of GeO_2. The estimated pressure sensitivity of this fiber was about 1.14 GHz/MPa with an accuracy of 3.5 kPa (i.e., an uncertainty of 4 MHz for the BDG frequency shift) up to 50 MPa. The Authors also performed an analysis of the sensitivity dependence on holes radii, the distance of holes from fiber center, and the percentage of doping, finding that the sensitivity is enhanced by increasing the radii of the holes and the holes-fiber center distance, while it gets decreased with the doping concentration.

Teng et al. [61] proposed to measure the hydrostatic pressure-induced birefringence changes by exciting and probing the BDGs in a thin-diameter 4 m-long pure silica polarization-maintaining photonic crystal fiber (PM-PCF). Thin diameter photonic crystal fibers are characterized by a holey structure that is more prone to deform under the external pressure and, therefore, the sensitivity to hydrostatic pressure is enhanced. Moreover, as for most PCFs, the all-silica solid core and the porous cladding have very similar thermal expansion coefficients and, therefore, the temperature-induced birefringence is expected to be reduced, at least for bare PM-PCFs [62]. Indeed, the BFS temperature coefficient of this fiber was estimated to be 1.0 MHz/°C. On the contrary, the BFS of this fiber resulted in being almost insensitive to the pressure, showing a variation of only 1.88 MHz in the range 0–1.1 Mpa. A sensitivity of 199 MHz/MPa was achieved by probing the change of birefringence by the BDGs, with a non-linear temperature-induced variation of the birefringence of about 176 MHz over the range −40–70 °C. To tackle the temperature crosstalk on the birefringence changes, the Authors firstly probed the BFS changes to obtain the temperature distribution along the fiber, and then the birefringence changes induced by both temperature and pressure. Next, the effect of the temperature was subtracted from the fiber birefringence according to the measured temperature distribution. Ultimately, with this pressure-sensing technique, the Authors achieved a temperature-compensated distributed measurement of hydrostatic pressure, with a maximum measurement error smaller than 30 kPa at a spatial resolution of 20 cm.

An extensive characterization of the sensitivity of dif-

ferent types of commercial PM fibers, interrogated by the optical time-domain analysis of BDGs, has been carried out by Kim et al. [63]. The fibers considered in this work were one PM-PCF, two Bow-tie fibers, and one Panda fiber, which have been interrogated over the range 0.1–6.1 MPa, with a spatial resolution ranging from 1 to 1.8 m. The pressure sensitivity of the BDG frequency has been measured to be −245.11, 94.27, 113.13 and 124.73 MHz/MPa for the PM photonic crystal fiber (PM-PCF), two Bow-tie fibers, and PANDA fiber, respectively. As one may note, the hydrostatic pressure tends to increase the BDG frequency (and the birefringence) of Bow-tie and Panda PMFs and to decrease it in the PM-PCF fiber. The accuracy of the measurement, limited primarily by the temperature fluctuations, was estimated at 0.008 MPa (i.e., ±2 MHz in the BDG frequency shift) for the PM-PCF and 0.064 MPa (i.e., ±6 MHz) for the last three fibers. The ameliorated accuracy of the PM-PCF comes again from the negligible temperature cross-sensitivity of this kind of fiber.

Again, the specifications of the DPSs mentioned above, exploiting the measurement of pressure-induced birefringence, are summarized in Table 2.

4. Measurement of pressure-induced losses in special optical fibers

We conclude this survey by mentioning the works based on the pressure-dependent losses in custom optical fibers. This approach, yet mediated by proper transducing mechanisms, has also been explored in single-point [64, 65] and quasi-distributed sensors [66, 67], but the most noticeable example of this class in distributed pressure sensing has been proposed by Zhou et al. [68], and consists of an optical fiber with soft cladding, made of silicone rubber, and a low-absorption silica core. The thickness and the refraction index of the cladding change significantly under pressure, leading to increased transmission losses. Upon proper pretreatment (i.e., a prior exposition to a pressure beyond the maximum range of use), a portion of 0.5 m of this fiber showed a sensibility in the order of 5 dB/MPa. This kind of approach, however, severely limits the maximum length over which the measurement can be done, in particular for broad pressure range. Furthermore, as other intensity-based sensing approaches, its accuracy and resolution are poor, being affected by other sources of loss (e.g. macro- and micro-bending) that may affect the measurement.

5. Conclusions

The first-ever proposed distributed pressure sensor can be dated back to 1980 when Rogers proposed to use the polarization of Rayleigh backscattered light to implement a fiber optic sensor to distributedly measure various physical fields along the fiber, among which the pressure was included. Since then, many works have addressed this problem, following different approaches. For completeness, we have tried to include as many references as possible in the bibliography.

In this review, we have covered different sensing mechanisms. Systems based on the distributed measurement of pressure-induced strain in compliant coated optical fibers and engineered cables have been investigated for a rather long time due to their simplicity. Furthermore, they can rely on commercial interrogators as the physical parameter directly measured is the strain, then transduced into pressure. This also represents their main drawback, as the strain cross-sensitivity cannot be tackled, except through a proper installation preventing extraneous strain not induced by the pressure field.

The approaches based on the measurement of pressure-induced birefringence in special optical fibers have been addressed since the very beginning and, in the years, have included different engineered fiber types and implementations of the interrogation optical setup. These implementations are often complex and not commercially available. Among the different fibers that are most promising, we can mention the PM-PCF, interrogated by exciting and probing the BDG center frequency, for their negligible temperature sensitivity, which, however, may suffer by a very complex optical setup, large losses as well as high cost.

Among the other more exotic approaches, the one exploiting distributed acoustic sensing scheme, still quite crude, is promising but limited to the measurement of pressure waves.

To conclude, almost all the works deal with not-cabled fibers, which are hard to be used in real applications. In this sense, whatever sensing mechanism is chosen, the effort of the research should be focused on developing distributed pressure sensors suitable for field applications. This also implies that the efforts should address cable engineering problems, including careful analysis of the material properties and the mechanical interaction with the pressure field. In this perspective, Ref. [41] provides a clear indication of the viability of this approach.

Acknowledgement

Partial support from the European Commission (Horizon 2020) and the Italian Ministry of Instruction, University and Research, within the Water JPI and the WaterWork2014 Cofunded Call (project DOMINO), is acknowledged.

The work is also partly supported by the Italian Ministry for Education, University and Research (MIUR, "Departments of Excellence" – law 232/2016, and PRIN 2017 – project 2017HP5K) and by the University of Padova (BIRD 2019 – project MACFIBER).

L.S. also acknowledges the "Regional Operational Program – European Regional Development Fund (ROF ERDF 2014-2020) of the Veneto Region, Axis 1 – Research, Technological Development and Innovation (ACTION 1.1.4 –

Table 2: Distributed pressure sensors exploiting the measurement of pressure-induced strain.

Ref.	Tech.	Distance		Fiber type	Pressure			
		Resol. [m]	Range [m]		Sensitivity [MHz/MPa]*	Resol. [MPa]*	Range [MPa]*	Accur. [kPa]
[48]	POTDR	1	75	SHF	$-0.294\,\mathrm{rad\,m^{-1}\,MPa^{-1}}$	n.a.	5	n.a.
[54]	POFDR	0.01	2	PM-PCF	−522	0.287	13.8	n.a.
				SHF	−1874	0.080		
[56]	POFDR	0.01	0.77	EPCF	−499	0.301	24	n.a.
				PCF	-394	0.381		
[58]	ϕ-OTDR	0.05	26.5	"butterfly" PCF	−2190 [$-66\,\mathrm{rad\,m^{-1}\,MPa^{-1}}$]	0.029	6.8	22
			48	"butterfly" PCF	−954 [$-28.6\,\mathrm{rad\,m^{-1}\,MPa^{-1}}$]	0.068	6.8	59
[59]	ϕ-OTDR	0.05	10	SHF	−6100	0.011	0.1	1.5
			1050	SHF	900	0.072	0.1	
[61]	BDG	0.02	4	PM-PCF	199	$< 0.02^{\dagger}$	1.05	30
[63]	BDG	1.8	37	Bow-tie	113.13	0.035	6.1	64
			20	Bow-tie	94.27	0.042	6.1	64
			223	Panda	124.73	0.032	6.1	8
			4.5	PM-PCF	−245.11	0.016	6.1	8

* Unless otherwise specified

† Inferred from the setup

Support to R&D activities for the development of new sustainable technologies, products and services – project INMOSTRA)".

References

[1] V. E. A. Post, J. R. von Asmuth, Review: Hydraulic head measurements—new technologies, classic pitfalls, Hydrogeol J 21 (4) (2013) 737–750. doi:10.1007/s10040-013-0969-0.

[2] S. P. Venkateshan, Measurement of Pressure, in: Mechanical Measurements, John Wiley & Sons, Ltd, 2015, pp. 243–279. doi:10.1002/9781119115571.ch7.

[3] S. Sikarwar, Satyendra, S. Singh, B. C. Yadav, Review on pressure sensors for structural health monitoring, Photonic Sens 7 (4) (2017) 294–304. doi:10.1007/s13320-017-0419-z.

[4] L. Liu, H. Zhang, Q. Zhao, Y. Liu, F. Li, Temperature-independent FBG pressure sensor with high sensitivity, Optical Fiber Technology 13 (1) (2007) 78–80. doi:10.1016/j.yofte.2006.09.001.

[5] A. Leal-Junior, A. Theodosiou, A. Frizera-Neto, M. J. Pontes, E. Shafir, O. Palchik, N. Tal, S. Zilberman, G. Berkovic, P. Antunes, P. André, K. Kalli, C. Marques, Characterization of a new polymer optical fiber with enhanced sensing capabilities using a Bragg grating, Opt. Lett., OL 43 (19) (2018) 4799–4802. doi:10.1364/OL.43.004799.

[6] L. Schenato, Q. Rong, Z. Shao, X. Qiao, A. Pasuto, A. Galtarossa, L. Palmieri, Highly-Sensitive FBG Pressure Sensor Based on a 3D-Printed Transducer, Journal of Lightwave Technology 37 (18) (2019) 1–6. doi:10.1109/JLT.2019.2919917.

[7] E. Vorathin, Z. M. Hafizi, N. Ismail, M. Loman, Review of high sensitivity fibre-optic pressure sensors for low pressure sensing, Optics & Laser Technology 121 (2020) 105841. doi:10.1016/j.optlastec.2019.105841.

[8] D. Abeysinghe, S. Dasgupta, J. Boyd, H. Jackson, A novel MEMS pressure sensor fabricated on an optical fiber, IEEE Photonics Technology Letters 13 (9) (2001) 993–995. doi:10.1109/68.942671.

[9] E. Pinet, A. Pham, S. Rioux, Miniature fiber optic pressure sensor for medical applications: An opportunity for intra-aortic balloon pumping (IABP) therapy, in: Bruges, Belgium - Deadline Past, Bruges, Belgium, 2005, p. 234. doi:10.1117/12.623806.

[10] Y. Zhao, Y. Liao, S. Lai, Simultaneous measurement of downhole high pressure and temperature with a bulk-modulus and FBG sensor, IEEE Photonics Technology Letters 14 (11) (2002) 1584–1586. doi:10.1109/LPT.2002.803914.

[11] X. Qiao, Z. Shao, W. Bao, Q. Rong, Fiber Bragg Grating Sensors for the Oil Industry, Sensors (Basel) 17 (3) (Feb. 2017). doi:10.3390/s17030429.

[12] C. M. Jewart, Q. Wang, J. Canning, D. Grobnic, S. J. Mihailov, K. P. Chen, Ultrafast femtosecond-laser-induced fiber Bragg gratings in air-hole microstructured fibers for high-temperature pressure sensing, Opt. Lett. 35 (9) (2010) 1443. doi:10.1364/OL.35.001443.

[13] H. Chikh-Bled, K. Chah, Á. González-Vila, B. Lasri, C. Caucheteur, Behavior of femtosecond laser-induced eccentric fiber Bragg gratings at very high temperatures, Opt. Lett., OL 41 (17) (2016) 4048–4051. doi:10.1364/OL.41.004048.

[14] J.-Y. Huang, J. V. Roosbroeck, J. Vlekken, A. B. Martinez, T. Geernaert, F. Berghmans, B. V. Hoe, E. Lindner, C. Caucheteur, FBGs written in specialty fiber for high pressure/high temperature measurement, Opt. Express, OE 25 (15) (2017) 17936–17947. doi:10.1364/OE.25.017936.

[15] L. Schenato, A Review of Distributed Fibre Optic Sensors for Geo-Hydrological Applications, Applied Sciences 7 (9) (2017) 896. doi:10.3390/app7090896.

[16] C. S. Baldwin, Applications for fiber optic sensing in the upstream oil and gas industry, in: G. Pickrell, E. Udd, H. H. Du (Eds.), SPIE Sensing Technology + Applications, Baltimore, Maryland, United States, 2015, p. 94800D. doi:10.1117/12.2176226.

[17] N. Lagakos, J. Bucaro, Phase-modulated fiber optic acoustic

sensors, ISA Transactions 28 (2) (1989) 1–6. doi:10.1016/0019-0578(89)90033-5.

[18] B. Budiansky, D. C. Drucker, G. S. Kino, J. R. Rice, Pressure sensitivity of a clad optical fiber, Applied optics 18 (24) (1979) 4085–4088.

[19] A. J. Rogers, Distributed optical-fibre sensors for the measurement of pressure, strain and temperature, Journal of the Institution of Electronic and Radio Engineers 58 (5) (1988) S113–S122. doi:10.1049/jiere.1988.0048.

[20] G. B. Hocker, Fiber-optic sensing of pressure and temperature, Applied Optics 18 (9) (1979) 1445. doi:10.1364/AO.18.001445.

[21] P. Shajenko, J. P. Flatley, M. B. Moffett, On fiber-optic hydrophone sensitivity, The Journal of the Acoustical Society of America 64 (5) (1978) 1286–1288. doi:10.1121/1.382113.

[22] J. A. Bucaro, T. R. Hickman, Measurement of sensitivity of optical fibers for acoustic detection, Appl. Opt., AO 18 (6) (1979) 938–940. doi:10.1364/AO.18.000938.

[23] J. A. Bucaro, H. D. Dardy, E. F. Carome, Fiber-optic hydrophone, The Journal of the Acoustical Society of America 62 (5) (1977) 1302–1304. doi:10.1121/1.381624.

[24] J. A. Bucaro, H. D. Dardy, E. F. Carome, Optical fiber acoustic sensor, Appl. Opt., AO 16 (7) (1977) 1761–1762. doi:10.1364/AO.16.001761.

[25] J. A. Bucaro, E. F. Carome, Single fiber interferometric acoustic sensor, Appl. Opt., AO 17 (3) (1978) 330–331. doi:10.1364/AO.17.000330.

[26] D. Burnett, Chung-Chun Ong, Shortening of submerged ocean cables due to hydrostatic pressure, IEEE Journal of Oceanic Engineering 12 (1) (1987) 281–288. doi:10.1109/JOE.1987.1145239.

[27] R. Hughes, J. Jarzynski, Static pressure sensitivity amplification in interferometric fiber-optic hydrophones, Appl. Opt. 19 (1) (1980) 98–107. doi:10.1364/AO.19.000098.

[28] N. Lagakos, T. Hickman, J. Cole, J. Bucaro, Optical fibers with reduced pressure sensitivity, Opt. Lett. 6 (9) (1981) 443–445.

[29] N. Lagakos, J. A. Bucaro, Pressure desensitization of optical fibers, Appl. Opt., AO 20 (15) (1981) 2716–2720. doi:10.1364/AO.20.002716.

[30] N. Lagakos, I. J. Bush, J. H. Cole, J. A. Bucaro, J. D. Skogen, G. B. Hocker, Acoustic desensitization of single-mode fibers utilizing nickel coatings, Opt. Lett., OL 7 (9) (1982) 460–462. doi:10.1364/OL.7.000460.

[31] N. Lagakos, E. Schnaus, J. Cole, J. Jarzynski, J. Bucaro, Optimizing fiber coatings for interferometric acoustic sensors, IEEE Journal of Quantum Electronics 18 (4) (1982) 683–689, conference Name: IEEE Journal of Quantum Electronics. doi:10.1109/JQE.1982.1071565.

[32] N. Lagakos, J. Jarzynski, J. H. Cole, J. A. Bucaro, Frequency and temperature dependence of elastic moduli of polymers, Journal of Applied Physics 59 (12) (1986) 4017–4031. doi:10.1063/1.336707.

[33] Z. Tang, S. Lou, X. Wang, W. Zhang, S. Yan, Z. Xing, Using Mode Coupling Mechanism in Symmetrical Triple-Core Photonic Crystal Fiber for High Performance Strain Sensing, IEEE J. Select. Topics Quantum Electron. 26 (4) (2020) 1–7. doi:10.1109/JSTQE.2019.2947615.

[34] A. Méndez, E. Diatzikis, Fiber Optic Distributed Pressure Sensor Based on Brillouin Scattering, in: Optical Fiber Sensors, OSA, Cancún, Mexico, 2006, p. ThE46. doi:10.1364/OFS.2006.ThE46.

[35] G. Zhang, H. Gu, H. Dong, L. Li, J. He, Pressure Sensitization of Brillouin Frequency Shift in Optical Fibers With Double-Layer Polymer Coatings, IEEE Sensors J. 13 (6) (2013) 2437–2441. doi:10.1109/JSEN.2013.2255270.

[36] S. Le Floch, P. Cambon, Study of Brillouin gain spectrum in standard single-mode optical fiber at low temperatures (1.4–370 K) and high hydrostatic pressures (1–250 bars), Optics Communications 219 (1) (2003) 395–410. doi:10.1016/S0030-4018(03)01296-3.

[37] H. Gu, H. Dong, G. Zhang, Y. Dong, J. He, Dependence of Brillouin frequency shift on radial and axial strain in silica optical fibers, Appl. Opt., AO 51 (32) (2012) 7864–7868. doi:10.1364/AO.51.007864.

[38] H. G. Haidong Gu, H. D. Huijuan Dong, G. Z. Guangyu Zhang, J. H. Jun He, N. X. Ning Xu, D. J. B. Douglas. J. Brown, Pressure dependence of Brillouin frequency shift in bare silica optical fibers, Chin. Opt. Lett. 10 (10) (2012) 100604–100606. doi:10.3788/COL201210.100604.

[39] Y. Mizuno, H. Lee, N. Hayashi, K. Nakamura, Hydrostatic pressure dependence of Brillouin frequency shift in polymer optical fibers, Appl. Phys. Express 11 (1) (2017) 012502. doi:10.7567/APEX.11.012502.

[40] M. Becker, T. Coleman, C. Ciervo, M. Cole, M. Mondanos, Fluid pressure sensing with fiber-optic distributed acoustic sensing, The Leading Edge 36 (12) (2017) 1018–1023. doi:10.1190/tle36121018.1.

[41] L. Schenato, A. Pasuto, A. Galtarossa, L. Palmieri, An Optical Fiber Distributed Pressure Sensing Cable With Pa-Sensitivity and Enhanced Spatial Resolution, IEEE Sensors Journal 20 (11) (2020) 5900–5908. doi:10.1109/JSEN.2020.2972057.

[42] J. M. Henault, J. Salin, G. Moreau, M. Quiertant, F. Taillade, K. Benzarti, S. Delepine-Lesoille, Analysis of the strain transfer mechanism between a truly distributed optical fiber sensor and the surrounding medium, in: Concrete Repair, Rehabilitation and Retrofitting III: 3rd International Conference on Concrete Repair, Rehabilitation and Retrofitting, ICCRRR-3, 3-5 September 2012, Cape Town, South Africa, CRC Press, 2012, p. 266.

[43] A. J. Rogers, Polarisation optical time domain reflectometry, Electronics Letters 16 (13) (1980) 489–490. doi:10.1049/el:19800341.

[44] A. J. Rogers, Polarization-optical time domain reflectometry: A technique for the measurement of field distributions, Appl. Opt., AO 20 (6) (1981) 1060–1074. doi:10.1364/AO.20.001060.

[45] L. Palmieri, L. Schenato, Distributed Optical Fiber Sensing Based on Rayleigh Scattering, The Open Optics Journal 7 (1) (2013) 104–127.

[46] H. M. Xie, K. Okamoto, P. Dabkiewicz, R. Ulrich, Side-hole fiber for fiber-optic pressure sensing, Opt. Lett. 11 (5) (1986) 333. doi:10.1364/OL.11.000333.

[47] J. Clowes, S. Syngellakis, M. Zervas, Pressure sensitivity of side-hole optical fiber sensors, IEEE Photon. Technol. Lett. 10 (6) (1998) 857–859. doi:10.1109/68.681509.

[48] A. J. Rogers, S. V. Shatalin, S. E. Kanellopoulos, Distributed measurement of fluid pressure via optical-fibre backscatter polarimetry, in: 17th International Conference on Optical Fibre Sensors, Vol. 5855, International Society for Optics and Photonics, 2005, pp. 230–233. doi:10.1117/12.623804.

[49] K. Chiang, D. Wong, Hydrostatic pressure induced birefringence in a highly birefringent optical fibre, Electron. Lett. 26 (23) (1990) 1952. doi:10.1049/el:19901263.

[50] K. Chiang, Pressure-induced birefringence in a coated highly birefringent optical fiber, Journal of Lightwave Technology 8 (12) (1990) 1850–1855, conference Name: Journal of Lightwave Technology. doi:10.1109/50.62882.

[51] K. Chiang, D. Wong, Design of highly birefringent fibers to optimize or minimize pressure-induced birefringence, IEEE Photonics Technology Letters 3 (7) (1991) 654–656, conference Name: IEEE Photonics Technology Letters. doi:10.1109/68.87944.

[52] M. Szpulak, T. Martynkien, W. Urbanczyk, Effects of hydrostatic pressure on phase and group modal birefringence in microstructured holey fibers, Appl. Opt. 43 (24) (2004) 4739. doi:10.1364/AO.43.004739.

[53] T. Nasilowski, T. Martynkien, G. Statkiewicz, M. Szpulak, J. Olszewski, G. Golojuch, W. Urbanczyk, J. Wojcik, P. Mergo, M. Makara, F. Berghmans, H. Thienpont, Temperature and pressure sensitivities of the highly birefringent photonic crystal fiber with core asymmetry, Appl. Phys. B 81 (2-3) (2005) 325–331. doi:10.1007/s00340-005-1900-8.

[54] T. Chen, Q. Wang, R. Chen, B. Zhang, C. Jewart, K. P. Chen, M. Maklad, P. R. Swinehart, Distributed high-temperature

pressure sensing using air-hole microstructural fibers, Opt. Lett. 37 (6) (2012) 1064. doi:10.1364/OL.37.001064.

[55] R. R. J. Maier, W. N. MacPherson, J. S. Barton, S. McCulloch, B. J. S. Jones, Distributed sensing using Rayleigh scatter in polarization-maintaining fibres for transverse load sensing, Meas. Sci. Technol. 21 (9) (2010) 094019. doi:10.1088/0957-0233/21/9/094019.

[56] R. M. Gerosa, J. H. Osório, D. Lopez-Cortes, C. M. B. Cordeiro, C. J. S. de Matos, Embedded-Core Optical Fiber for Distributed Pressure Measurement Using an Autocorrelation OFDR Technique, in: 2019 Conference on Lasers and Electro-Optics (CLEO), 2019, pp. 1–2. doi:10.1364/CLEO_SI.2019.SF3L.2.

[57] M. E. Froggatt, D. K. Gifford, S. Kreger, M. Wolfe, B. J. Soller, Characterization of Polarization-Maintaining Fiber Using High-Sensitivity Optical-Frequency-Domain Reflectometry, J. Lightwave Technol. 24 (11) (2006) 4149–4154. doi:10.1109/JLT.2006.883607.

[58] S. Mikhailov, L. Zhang, T. Geernaert, F. Berghmans, L. Thévenaz, Distributed Hydrostatic Pressure Measurement Using Phase-OTDR in a Highly Birefringent Photonic Crystal Fiber, Journal of Lightwave Technology 37 (18) (2019) 4496–4500. doi:10.1109/JLT.2019.2904756.

[59] L. Zhang, Z. Yang, Ł. Szostkiewicz, Ł. Szostkiewicz, K. Markiewicz, T. Nasilowski, L. Thévenaz, Fully distributed pressure sensing with ultra-high-sensitivity using side-hole fibers, in: 26th International Conference on Optical Fiber Sensors (2018), Paper WF13, Optical Society of America, 2018, p. WF13. doi:10.1364/OFS.2018.WF13.

[60] S. N. Jouybari, H. Latifi, Z. Chenari, Distributed pressure measurement by Brillouin scattering dynamic grating for a two side holes fiber, in: Y. Liao, W. Jin, D. D. Sampson, R. Yamauchi, Y. Chung, K. Nakamura, Y. Rao (Eds.), OFS2012 22nd International Conference on Optical Fiber Sensor, Beijing, , China, 2012, pp. 84219A–84219A–4. doi:10.1117/12.964410.

[61] L. Teng, H. Zhang, Y. Dong, D. Zhou, T. Jiang, W. Gao, Z. Lu, L. Chen, X. Bao, Temperature-compensated distributed hydrostatic pressure sensor with a thin-diameter polarization-maintaining photonic crystal fiber based on Brillouin dynamic gratings, Opt. Lett. 41 (18) (2016) 4413. doi:10.1364/OL.41.004413.

[62] Y. H. Kim, K. Y. Song, Characterization of Nonlinear Temperature Dependence of Brillouin Dynamic Grating Spectra in Polarization-Maintaining Fibers, Journal of Lightwave Technology 33 (23) (2015) 4922–4927, conference Name: Journal of Lightwave Technology. doi:10.1109/JLT.2015.2495359.

[63] Y. H. Kim, H. Kwon, J. Kim, K. Y. Song, Distributed measurement of hydrostatic pressure based on Brillouin dynamic grating in polarization maintaining fibers, Opt. Express, OE 24 (19) (2016) 21399–21406. doi:10.1364/OE.24.021399.

[64] L. Rippert, J.-M. Papy, M. Wevers, S. Van Huffel, Fiber optic sensor for continuous health monitoring in CFRP composite materials, in: V. S. Rao (Ed.), SPIE's 9th Annual International Symposium on Smart Structures and Materials, San Diego, CA, 2002, pp. 312–323. doi:10.1117/12.475228.

[65] A. Leal-Junior, V. Campos, A. Frizera, C. Marques, Low-cost and high-resolution pressure sensors using highly stretchable polymer optical fibers, Materials Letters 271 (2020) 127810. doi:10.1016/j.matlet.2020.127810.

[66] S.-H. Jung, D.-H. Lee, K.-H. Kwon, J.-W. Song, Water sensor using macrobending-sensitive fiber for real-time submersion monitoring, Optics Communications 260 (1) (2006) 105–108. doi:10.1016/j.optcom.2005.10.043.

[67] L. Ribeiro, J. Rosolem, D. Dini, C. Floridia, C. Hortencio, E. Da Costa, E. Bezerra, R. De Oliveira, M. Loichate, A. Durelli, Fiber optic bending loss sensor for application on monitoring of embankment dams, in: SBMO/IEEE MTT-S International Microwave and Optoelectronics Conference Proceedings, 2011, pp. 637–641. doi:10.1109/IMOC.2011.6169273.

[68] B. Zhou, L. Htein, Z. Liu, A. P. Zhang, H.-y. Tam, Novel soft-cladding optical fiber for distributed pressure sensing, in: 2016 21st OptoElectronics and Communications Conference (OECC) Held Jointly with 2016 International Conference on Photonics in Switching (PS), 2016, pp. 1–3.